A Crystal Routine for Collimation Studies in Circular Proton Accelerators

D. Mirarchi[a,b], G. Hall[b], S. Redaelli[a], W. Scandale[a]

[a] *CERN, European Organization for Nuclear Research, CH-1211 Geneva 23, Switzerland*
[b] *Blackett Laboratory, Imperial College, London SW7 2AZ, United Kingdom*

Abstract

A routine has been developed to simulate interactions of protons with bent crystals in a version of `SixTrack` for collimation studies. This routine is optimized to produce high-statistics tracking simulations for a highly efficient collimation system, like the one of the CERN Large Hadron Collider (LHC). The routine has recently been reviewed and improved through a comparison with experimental data, benchmarked against other codes and updated by adding better models of low-probability interactions. In this paper, data taken with 400 GeV/c proton beams at the CERN-SPS North Area are used to verify the prediction of the routine, including the results of a more recent analysis.

Keywords: LHC, SPS, H8, collimation, crystals, UA9, `SixTrack`

1. Introduction

In large accelerating machines such as the Large Hadron Collider (LHC), the prediction of how particle losses are distributed around the whole ring is crucial. This is performed at CERN using a `SixTrack` version for collimation studies [1]-[5]. A routine to simulate interactions of protons with bent crystals was also added for crystal collimation studies [6]. This routine is based on a Monte-Carlo approach, and the proton interactions with crystals are randomly sampled using probability distributions, as opposed to other tools [7] that integrate the proton motion in the crystalline potential. The routine is therefore optimized for high statistics runs, without jeopardizing because the known interactions with bent crystals are modelled accurately in the literature, and the few free parameters can be tuned on experimental data.

The crystal routine is composed of two main blocks with interplay between them: one contains models to describe coherent interactions in a bent crystal, and a scattering routine that describes interactions with amorphous materials. The scattering routine, recently updated to take into account LHC measurements [8], is called each time a proton does not experience a coherent process in bent crystals. The same scattering routine is also applied to particles trapped between crystalline planes, but with cross sections rescaled by the average nuclear density seen during their path [9]. Thus, the possibility of such protons also to experience nuclear interactions [14] is now taken into account. The coherent processes in bent crystals modelled are channeling, dechanneling, volume reflection, volume capture and dechanneling after volume capture. The models used are extensively discussed in [9], and based on work reported in [10]-[14]. Possible crystal imperfections were also introduced, such as the presence of an amorphous layer and the miscut angle [6]. The benchmarking with respect to experimental data of such a crystal routine is discussed.

2. Single-pass measurements

The experimental measurements have been performed with 400 GeV/c proton beams at the CERN-SPS North Area, in the framework of the UA9 collaboration. A total of 26 crystals was tested in the runs between 2009 and 2012. After detailed analysis of all the data collected during those years, a subset of 10 crystals was chosen for comparative studies with simulation routines [15, 16]. Among those ten crystals, a specific reference case was used to benchmark all the existing simulation codes for bent crystals developed in the framework of the UA9 collaboration, during "The 6th International Conference - Channeling 2014" [17]. The benchmarking described below refers to such a crystal, which is a silicon strip crystal 2 mm long and with 13.9 m bending radius. Besides the code discussed in this paper (`CRYCOLL`), other crystal routines involved in these comparisons are based on integration of an equation of motion in crystalline potential (`CRYD`) [7], and implementation of a crystal geometry in `FLUKA` [18] and `GEANT4` [19]. An overview of results obtained by the different codes can be found in [20]. Other simulation codes are available [21] which are not included in the present comparisons.

An example of a high statistics run in optimal channeling orientation for this crystal is given in the top graph of Fig. 1, while the middle and bottom graphs of Fig. 1 refer to simulation results. From these plots the effect of the experimental resolution on the agreement between experimental and simulated data is clearly visible. The experimental resolution is taken into account by adding random gaussian noise with $\sigma \sim 5\ \mu$rad to the simulated deflections, which corresponds to the measured resolution of the telescope used [22]. Simulation data are generated in a format that mimics the measured data format in order to apply the same analysis tools developed and used in [15, 16, 23]. This ensures a consistent treatment of simulation results and measurement data.

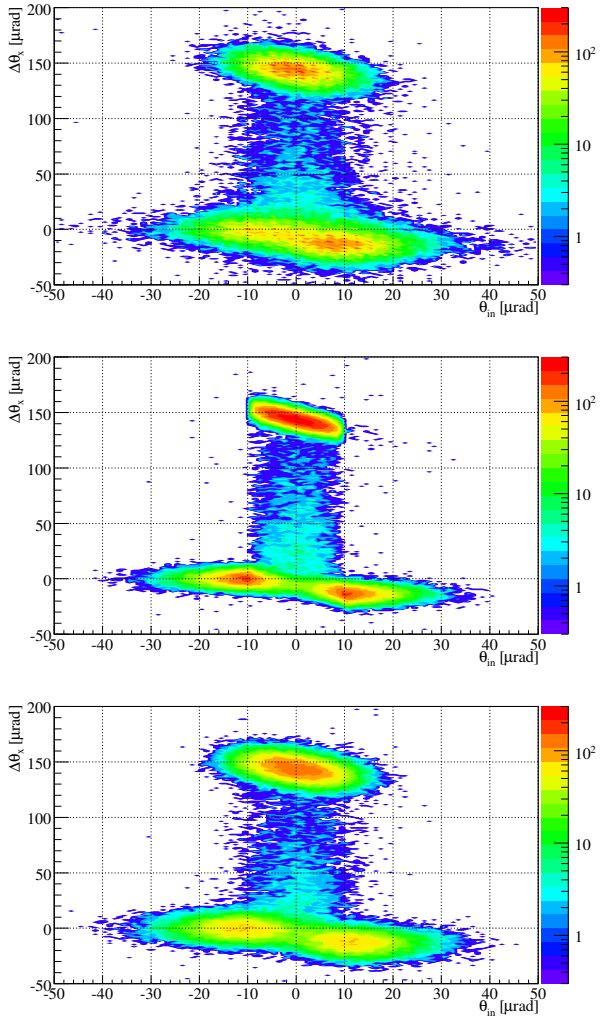

Figure 1: Angular deflection given to each particle as a function of the incident angle with respect to crystalline planes, during a high statistics run. (top) experimental data, (middle, bottom) simulated data without, and including, the experimental resolution, respectively.

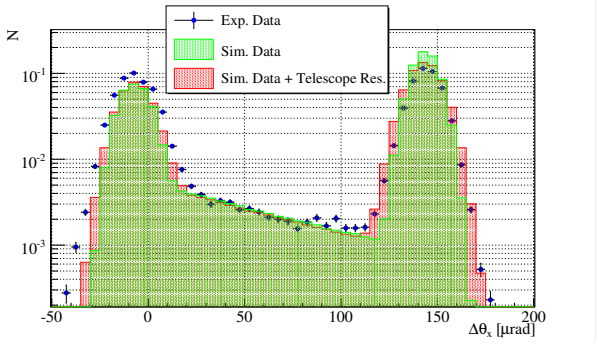

Figure 2: Distribution of deflections given to protons with an incoming angle within $\pm 10 \mu$rad. Experimental data are reported in blue dots with their statistical error, simulated data are shown in green, and their convolution with the telescope resolution is given in red. The binning of 5 μrad is chosen according to the experimental resolution, and histograms are normalized to the total number of entries.

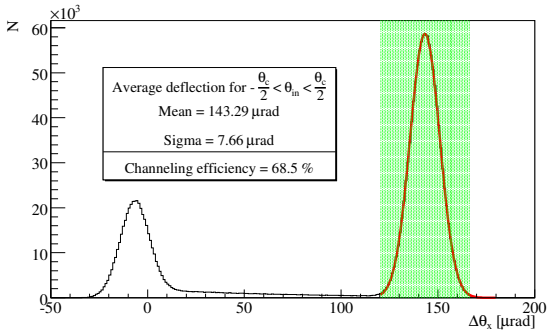

Figure 3: Simulated distributions of angular deflections given by the crystal. The angular range in which protons are considered as channeled is highlighted in green.

3. Qualitative comparison

In this section a qualitative overview of measured and simulated data, for the high statistics run in Fig. 1, is given. A ± 10 μrad cut on the proton incident angle is applied, and the distributions of deflections obtained are superimposed in Fig. 2. All are normalized to the total number of entries. It is possible to evaluate the agreement between:

- Distribution of channeled particles, both on the mean and width when the telescope resolution is taken into account.
- Distribution of particles in the transition regions, i.e. deflections close to zero, both on the mean and width when the experimental resolution is taken into account.
- Distribution of dechanneled particles, where experimental and simulated data match very well, with and without the telescope resolution.

The relative height of these distributions shows that the assumptions used to model the channeling efficiency and the coherent processes in bent crystals, are qualitatively adequate. In the selected angular range of the incoming protons the processes of channeling, dechanneling, volume reflection, and amorphous orientation occur simultaneously. A detailed analysis of these data for each of the items above follows.

4. Channeling efficiency

One of the key observables to be reproduced by crystal simulation routines is the channeling efficiency for a given bending radius. The channeling efficiency is a quantity used to define the fraction of particles undergoing channeling, normalised to the total number of particles impinging on the crystal within a given angular range. This cut on the angle of incident protons is needed to avoid any feature due to particles that cannot be channeled in any case (i.e. angles above the critical channeling value), as well as to decouple different interaction regimes as shown in the next sections.

The angular range in which particles are considered as channeled is calculated as the centroid of channeled peak within $\pm 3\sigma$ of the centre of the peak [16, 23], and shown by the green

Table 1: Measured and simulated channeling efficiency, for different angular cuts, with and without the experimental resolution taken into account.

Data	Cut [μrad]	Resolution	CH eff. [%]
Exp.	5	-	68.9
Sim.	5	no	78.4
Sim.	5	yes	68.5
Exp.	10	-	54.0
Sim.	10	no	63.9
Sim.	10	yes	60.8

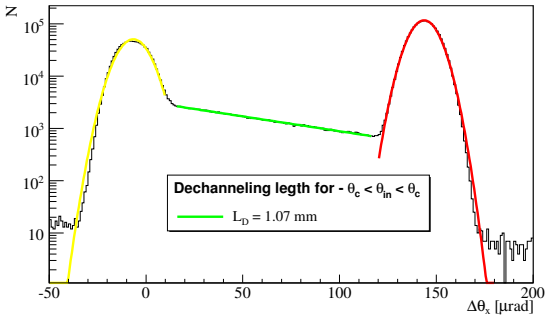

Figure 4: Simulated distribution of angular deflections given by the crystal. The dechanneling length is measured through the exponential fit in green. Same data as in Fig. 2 are used, but with binning of 1 μrad.

area in Fig. 3. This analysis was made using two different values of θ_{cut} on the proton incident angle, connected to the critical channeling angle (θ_c). They are equal to 5 μrad and 10 μrad, i.e. $\sim\theta_c/2$ and $\sim\theta_c$, respectively, at 400 GeV/c. What is shown in Fig. 3 refers to an angular cut of $\theta_{\text{cut}} = 5\mu$rad. The experimental resolution is also taken into account as described previously.

A complete overview of the channeling efficiency obtained for the two different angular cuts, both with and without the experimental resolution, is given in Table 1. An agreement within $\sim$10% is obtained when the telescope resolution is not taken into account, and $\sim$5% when it is convoluted with simulation results. The former case without resolution, though less relevant for the benchmarking, is shown for comparison with other simulation tools.

5. Dechanneling length

Like the channeling efficiency, the characteristic dechanneling length is a key feature for reliable description of coherent interactions in bent crystals. It can be modelled as an exponential decay of the initial population of trapped particles between crystalline planes [10], with electronic and nuclear dechanneling lengths needed to describe the whole process [9]. The electronic dechanneling length is calculated analytically for each proton initially trapped, using a formula based on the theoretical approach in [10]. The only free parameter is the scaling factor to extrapolate the characteristic nuclear dechanneling length from the electronic one, because an analytical formula is not yet available in the literature. The nuclear dechanneling length is applied only to the 10 % of protons initially trapped

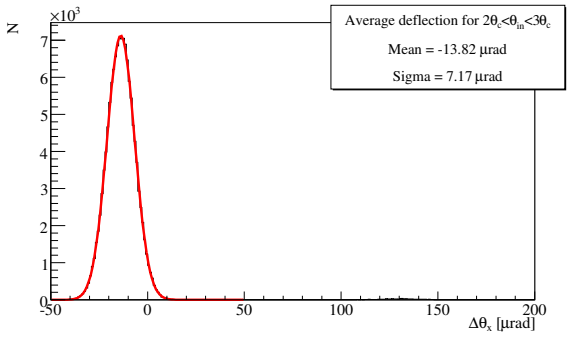

Figure 5: Simulated distribution of angular deflections given by the crystal to particles undergoing volume reflection.

Table 2: Mean deflection and angular spread of protons undergoing volume reflection.

Data	Resolution	Mean [μrad]	σ [μrad]
Exp.	-	-14.0	8.0
Sim.	no	-13.9	5.1
Sim.	yes	-13.8	7.2

between crystalline planes[1]. Fine tuning of this scaling factor was performed and what is obtained using an angular cut of $\theta_{\text{cut}} = 10\,\mu$rad is shown in Fig. 4. Similar results are obtained for $\theta_{\text{cut}} = 5\,\mu$rad.

The total dechanneling length is estimated from an exponential fit in a defined angular range, as described in [16, 23]. The decay constant of the exponential fit in green in Fig. 4 multiplied by the crystal bending radius gives the dechanneling length (L_D). The measured length is equal to $L_D \sim$1.23 mm [16] and the simulated value is $L_D \sim$1.07 mm; thus agreement at the $\sim$90% level is found. Convolution with the experimental resolution is not performed in this case, since it does not have a significant impact on the population of particles, as can be clearly seen from Fig. 2.

6. Volume reflection

A realistic description of this process is crucial for our purpose of crystal-assisted collimation. Particles undergoing such a process will acquire a deflection that is not large enough to reach the next collimation stage and will keep circulating in the machine. The key parameters that show the validity of the volume reflection model implemented in the routine are the deflection and angular spread given to the particles. They are analytically calculated for each proton undergoing this process using formulae based on the theoretical approach in [11, 12, 13].

Although analytical expressions can lead to distributions that different significantly from a gaussian, in this specific case mean deflection and spread can be measured through a gaussian fit of the deflections experienced by particles impinging

[1] Because the ratio between the with of a crystalline plane with respect to the interplanar distance is of about 10 %, in silicon strip crystals.

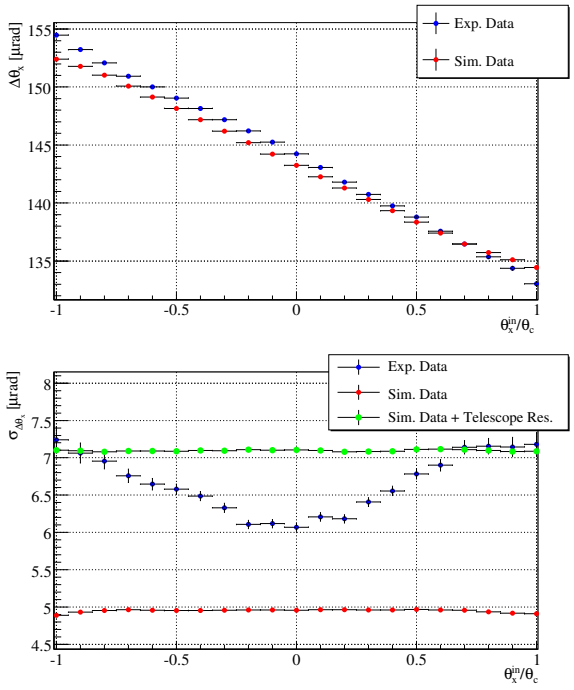

Figure 6: (top) Mean deflection given to particles channeled for the whole crystal length as a function of the incoming angle nomalized to the critical one, where measured and simulated data are shown in blue and red dots, respectively. (bottom) Angular spread of such particles, where simulated data convoluted with the experimental resolution are also shown (green dots).

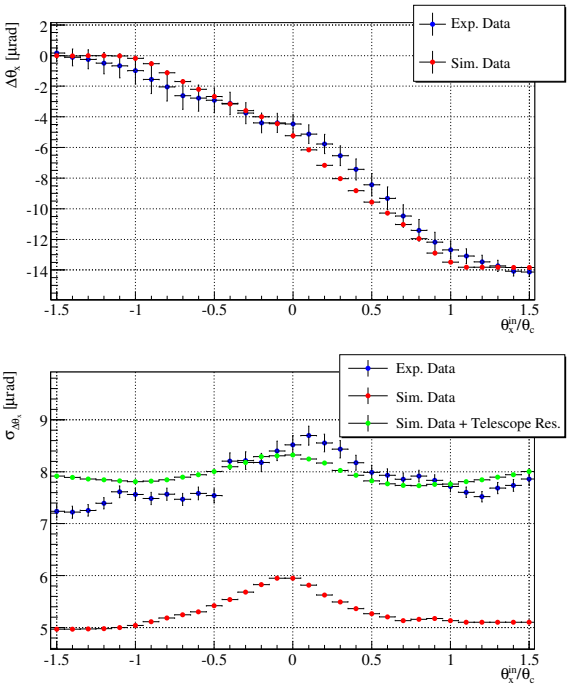

Figure 7: (top) Mean deflection given to particles in the transition from AM to VR process, as a function of the incoming angle normalized to the critical angle, where experimental and simulated data are shown in blue and red dots, respectively. (bottom) Angular spread of such particles, where simulated data convoluted with the experimental resolution are also shown (green dots).

on crystals with an angle in the range $2\theta_c < \theta_{in} < 3\theta_c$, i.e. $20\mu\text{rad} < \theta_{\text{in}} < 30\mu\text{rad}$ in Fig. 1. Simualtion results, convoluted with the experimental resolution, are shown in Fig. 5. However, what really matters in multiturn simulations is the spread obtained without such a convolution. A complete overview of what is obtained experimentally, with and without the telescope resolution, is given in Table 2, where results of the other routines involved in the comparisons are also reported.

7. Transition regions

In this section a comparative analysis of deflections given to particles channeled for the whole crystal length, and not trapped at all, is given.

We begin from deflections given to particles undergoing channeling. This analysis is performed by slicing into 2 μrad intervals the deflections given to particles incident on the crystal with $-\theta_c < \theta_{in} < \theta_c$, and performing a gaussian fit to those populations, as explained in [23]. The main outcome is to measure the average deflection and spread given to channeled particles, as shown in Fig. 6 top and bottom, respectively. Very good agreement is obtained in the comparison between experimental and simulated data regarding the mean deflection. Regarding the angular spread, a reduction of the width is observed experimentally for those entering the interplanar space with an angle close to zero, but not in the simulated data. This could be explained by reduced multiple Coulomb scattering as a result of the lower electronic density in the middle of the crystalline channel. For particles experiencing large oscillations, i.e. entering between the crystalline planes with an angle close to θ_c, the measured width is well reproduced by the simulated data, when convolution with the experimental resolution is taken into account. This discrepancy is due to the intrinsic nature of the simulation routine; the outgoing angle of particles flagged as channeled has no dependence on the angle of incidence, but is generated according to a gaussian distribution with constant width that depends on θ_c. This feature has negligible impact on collimation studies since all these particles will be captured by the next collimation stage.

We move now to particles that are not trapped between crystalline planes. They undergo interactions ranging from those experienced in amorphous silicon (AM, for $\theta_{in} < -\theta_c$) to full VR (for $\theta_{in} > \theta_c$), through a transition region where the two processes overlap. The trend with incident angle of the experimental values of mean deflection and angular spread was compared with simulated data, as shown in Fig. 7 top and bottom, respectively. Very good agreement was obtained for the mean deflection, in the whole transition region between full AM and full VR. The angular spread also agrees, when the experimental resolution is taken into account. Moreover, the growth of the spread for particles incident with an angle close to zero is also well reproduced, and can be explained by the convolution of the AM and VR processes.

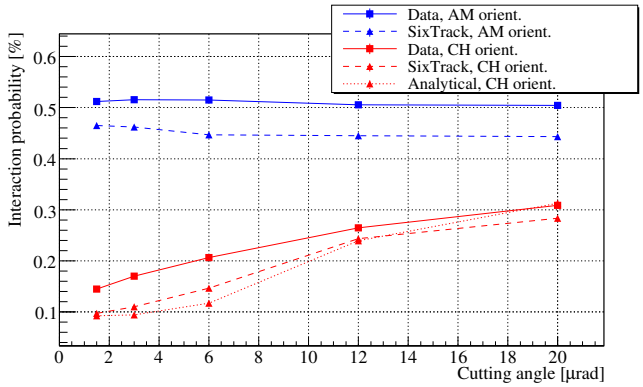

Figure 8: Probability of inelastic nuclear events as a function of the cut angle of protons incident on the crystal: data taken in AM orientation are shown in blue, where solid and dashed lines refer to experimental and simulated data respectively; data in CH orientation are shown in red, where solid and dashed lines refer to experimental and simulated data respectively. The dotted red line shows what was obtained by Taratin with the crystal routine described in [7], as reported in [14].

8. Nuclear interaction rate

One of the most significant tests of the validity of models implemented in simulation code is to reproduce events with very low probability. The best observable for our purpose is to check the rate of inelastic nuclear events in bent crystals, as a function of the angle of the incident protons. It is worthy of note that such interactions are the most dangerous for applications of crystals in the process of beam collimation, because they are the main source of off-momentum particles that can be lost at dispersive peaks around the machine.

This quantity can be measured by examining experimental observations reported in [14]. The same experimental conditions and data analysis were applied to the simulation performed with the routine in `SixTrack`. The probability of deep inelastic and single diffractive events was estimated as a function of a "cutting angle" on the incident protons[2]. Experimental data and simulations reported in [14] are superimposed on what is obtained with the routine in `SixTrack` in Fig. 8. As expected, a flat interaction probability is observed when the crystal behaves as an amorphous material. However, a difference of up to 20% between measured and simulated data is present, which is due to approximations used to determine the inelastic cross-section. As reported in [14], using the Glauber approximation a cross-section of $\sigma = 0.504$ b is obtained. Multiplying by the atomic density of silicon, $\rho = 0.05 \times 10^{24}\text{cm}^{-3}$, and the crystal length, $l = 1.94$ mm, $P = 0.49\%$ is obtained. In `SixTrack` approximations reported in the P.D.G. [24] are implemented, consistent with what is used to treat interactions in standard collimators [8]. These approximations give $\sigma = 0.430$ b, that implies $P = 0.42\%$. In conclusion this discrepancy is understood and under control, since it does not have a significant effect for our purpose and is not linked to the modelling of coherent processes in bent crystals.

[2] i.e. all protons incident with an angle below the cut are considered.

Much more interesting for our needs is what is reported in red in Fig. 8, which shows the interaction probability when the crystal is placed in the optimal channeling orientation. The solid line refers to experimental results, the dotted line shows simulation output from code that solves the equation of motion in the crystalline potential as described in [7], and simulation results obtained using the routine in `SixTrack` are shown by the dashed line. Although good agreement is found between the two simulation codes over the whole angular range, both of them have a discrepancy with respect to measurements for small incident angle. This could be explained by small variations of the crystal angle during data taking, which required about 24h, as thermal variations could affect the mechanism of the goniometer which supported the crystal. Further analysis of this discrepancy and its explanation is reported in [14].

9. Conclusions

The benchmarking of the crystal routine in `SixTrack`, performed with respect to experimental data taken with 400 GeV/c proton beams at the CERN-SPS North Area, is discussed. A qualitative comparison shows good agreement on the entire set of data for an high-statistics run in optimal channeling orientation. Detail studies demonstrated agreement within the 5% compared to the measured channeling efficiency. The dechanneling length was optimized to reproduce the measured behaviour at the level of 90%. The mean deflection and angular spread of particles undergoing volume reflection, channeling and in the transition region from full AM to full VR is also reproduced with a high level of accuracy. The nuclear interaction rate in optimal channeling orientation agrees with data in literature. This makes us confident of the predictions that can be made with such a routine in multiturn tracking simulation of a circular proton accelerator.

10. Acknowledgments

The authors thank the whole UA9 collaboration which collected the experimental data, and the LHC collimation team in the CERN-ABP group for the simulation tools provided. In particular I. Yazynin who first developed the routine and V. Previtali implemented it in `SixTrack`, under the supervision of R. Assmann. R. Rossi for the analysis of the raw data, and A. Taratin for useful discussions. Work supported by EU FP7 HiLumi LHC - Grant Agreement 284404, and UK Science and Technology Facilities Council.

[1] F. Schmidt. "Sixtrack, user reference manual." CERN, 1994, SL/94-56.
[2] G. Robert-Demolaize et al., "A new version of SixTrack with collimation and aperture interface", PAC05, Knoxville, TN, USA, 2005.
[3] http://lhc-collimation-project.web.cern.ch/lhc-collimation-project/code-tracking-2012.php
[4] R. Assmann et al., "Tools for predicting cleaning efficiency in the LHC", PAC03, Portland, OR, USA, 2003.
[5] S. Redaelli et al., "LHC aperture and commissioning of the collimation system", LHC Project Workshop "Chamonix XIV", January 2005.
[6] V. Previtali, "Performance evaluation of a crystal-enhanced collimation system for the LHC", CERN-THESIS-2010-133
[7] A.M. Taratin, "Particle channeling in a bent crystal", Phys.Part.Nucl. 29 (1998) 437-462, Fiz.Elem.Chast.Atom.Yadra 29 (1998) 1063-1118

[8] C. Tambasco et al., “Improved physics model for collimation tracking studies at LHC”, to be published.
[9] D. Mirarchi, “Crystal collimation for LHC”, PhD thesis, under preparation.
[10] V.M. Biryukov, Y.A. Chesnokov, V.I. Kotov., “Crystal channeling and its application at high energy accelerators”, Springer, 1996.
[11] W. Scandale et al., “Volume Reflection Dependence of 400 GeV/c Protons on the Bent Crystal Curvature”, Phys. Rev. Lett. 101 (2008) 234801
[12] A. M. Taratin, W. Scandale, “Volume reflection of high-energy protons in short bent crystals”, NIM B 262 (2007) 340-347
[13] Y.A. Chesnokov et al., “Volume capture and volume reflection of ultrarelativistic particles in bent single crystals”, arXiv:0808.1486
[14] W. Scandale et al., “Probability of inelastic nuclear interactions of high-energy protons in a bent crystal”, NIM B 268 (2010) 2655-2659
[15] http://lhc-collimation-upgrade-spec.web.cern.ch/LHC-Collimation-Upgrade-Spec/H8-input.php
[16] R. Rossi et al., “Measurements of coherent interactions of 400 GeV proton in silicon bent crystals”, submitted to NIM B
[17] http://www.lnf.infn.it/conference/channeling2014/main.php
[18] P. Schoofs et al., “FLUKA event generator for crystal channeling”, Channeling 2014, Capri.
https://agenda.infn.it/getFile.py/access?contribId=86&sessionId=19&resId=0&materialId=slides&confId=7409
[19] E. Bagli et al., “GEANT4 channeling”, Channeling 2014, Capri.
https://agenda.infn.it/getFile.py/access?contribId=16&sessionId=19&resId=0&materialId=slides&confId=7409
[20] F. Galluccio et al., “Summary on crystal simulation routines for particle accelrators”, Channeling 2014, Capri.
https://agenda.infn.it/getFile.py/access?contribId=233&sessionId=20&resId=0&materialId=slides&confId=7409
[21] A. Babaev and S. Dabagov, “Simulations of planar channeling of relativistic nuclei in a bent crystal”, The European Physical Journal Plus 127:62 (2012)
[22] M. Pesaresi et al., “Design and performance of a high rate, high angular resolution beam telescope used for crystal channeling studies”, 2011 JINST 6 P040006.
[23] R. Rossi, “Measurements of coherent interaction phenomena on bent crystal for the LHC at 400 GeV”, CERN-THESIS-2014-187
[24] http://pdg.lbl.gov